

Reactions of Chlorine with Liquid Metals. 3. Bismuth

M. Balooch,[†] W. J. Siekhaus,[‡] and D. R. Olander^{†*}

Materials and Molecular Research Division of the Lawrence Berkeley Laboratory and Department of Nuclear Engineering, University of California, Berkeley, California 94720, and Chemistry Division of the Lawrence Livermore National Laboratory, Livermore, California 94550 (Received: August 22, 1985)

The reaction of molecular chlorine with solid and liquid bismuth was studied by modulated molecular beam-mass spectrometric methods over the temperature range 400–800 K and equivalent chlorine pressures of 5×10^{-6} – 2×10^{-4} torr. The sole reaction product with solid Bi(0001) was BiCl_3 . This species disappeared at the melting point. The molecular beam data collected on the trichloride product exhibited nonlinearity and evidence of both branched and series processes in the mechanism. These results, in conjunction with data obtained in a prior investigation of the system by thermal desorption spectroscopy, permitted development of a model of the reaction on the surface of the solid. With liquid bismuth, only BiCl was detected as reaction product. Its reaction probability increased with temperature, most likely because of a corresponding increase in the chlorine sticking probability. The 45° phase lag exhibited by this species indicated that the kinetics were dominated by solution and diffusion of chlorine in the bulk liquid bismuth.

I. Introduction

In the first two parts of this series,^{1,2} the kinetics and mechanisms of the indium-chlorine and lead-chlorine reactions were investigated by the modulated molecular beam technique in temperature ranges bracketing the solid-liquid-phase transformations. Pronounced changes in the reactivity of the metals to chlorine were observed as the melting point was crossed, but the changes could not be described as discontinuities.

The present work is an extension of this type of gas-liquid and gas-solid reaction study to the bismuth-chlorine system. Recently, Campbell and Taylor³ reported the results of an investigation of the $\text{Cl}_2/\text{Bi}(0001)$ reaction to 500 K using LEED, AES, and thermal desorption spectroscopy (TDS). The availability of these data provides an opportunity to compare a reaction model deduced from modulated molecular beam data with one obtained by an entirely different surface reaction detection technique. A separate AES study of the Bi/Cl_2 system was not undertaken (as had been done for the indium and lead reactions) because of the extensive surface analytical results reported by Campbell and Taylor.³

II. Experimental Section

The experimental approach has been described in detail in the first part of this series.¹ To review the method, a beam of molecular chlorine is formed by effusion from a glass source tube, mechanically modulated, and collimated to 1-mm diameter before striking the bismuth target. The latter is mounted in a horizontal position in a molybdenum crucible located in a separate reaction chamber. This arrangement permits the reaction to be investigated with solid or liquid bismuth without the necessity of breaking the vacuum or otherwise changing reaction conditions.

Scattered chlorine and volatile bismuth chloride products of the surface reaction are detected by a quadrupole mass spectrometer located in the third chamber, which communicates with the chamber housing the metal target via a 1-mm-diameter orifice. The output from the mass spectrometer is processed by a lock-in amplifier to provide the amplitude and phase of the product signals relative to that of the chlorine reactant beam incident on the target. The surface temperature (measured by an infrared pyrometer), the reactant beam intensity, and the modulation frequency are the experimental variables.

Initially the surface exposed to the chlorine beam is the (0001) face of a bismuth single crystal of 99.99% purity. Prior to placement in the apparatus, the specimen is ultrasonically rinsed

in trichloroethylene, acetone, and ethanol. In the vacuum chamber, the surface is cleaned by repeated argon ion bombardment and annealing at 510 K. All experiments on the liquid surface were performed after completion of data acquisition on the solid phase.

III. Results

The bismuth-containing ions observed by the mass spectrometer with the solid target were Bi^+ , BiCl^+ , BiCl_2^+ , and BiCl_3^+ . All had the same phase angle and the same dependence on surface temperature. This behavior indicates that all were part of the cracking pattern of BiCl_3 , which is therefore the sole volatile product of chlorine with solid bismuth. This result is in agreement with that reported by Campbell and Taylor.³ All measurements were made on the BiCl_2^+ peak, which has the highest intensity, and then corrected for the fragmentation pattern to produce a measure of the BiCl_3 emission rate from the surface.

The only ions observed for the liquid-phase reaction were BiCl^+ and Bi^+ , of comparable magnitudes. Both exhibited the same phase angle and the same dependence on surface temperature, demonstrating their origin as BiCl . This species is thus the sole volatile reaction product of chlorine and liquid bismuth.

In order to convert the mass spectrometer signals (after correcting for fragmentation) to reaction probabilities, estimates of the ratios of the total ionization cross sections of BiCl_3 or BiCl to that of Cl_2 reaction are needed. Inasmuch as none of these have been measured, the estimates were based on the additivity rule⁴ using cross sections of the atoms.⁵ In addition, the measured phase angles of products and the scattered reactant were corrected for different transit times between the surface and the detector by using the method of Harrison et al.⁶

The experimental results are plotted in Figures 1–7. The curves on these plots are the results of fitting the data to the reaction model discussed in sections IV and V.

Figure 1 shows measured reaction probabilities and phase lags for the BiCl_3 and BiCl products of the reaction with solid and liquid bismuth, respectively, as functions of surface temperature. The BiCl_3 signal at first increases rapidly with temperature but drops very sharply as the melting point is approached. The phase lag for this species is quite large (approaching 90° at low temperatures), which means that the associated apparent reaction probability is highly demodulated.⁷ Thus, the apparent reaction

(1) M. Balooch, W. J. Siekhaus, and D. R. Olander, *J. Phys. Chem.*, **88**, 3522 (1984).

(2) M. Balooch, W. J. Siekhaus, and D. R. Olander, *J. Phys. Chem.*, **88**, 3530 (1984).

(3) C. T. Campbell and T. N. Taylor, *Surf. Sci.*, **122**, 119 (1982).

(4) J. W. Otvos and D. P. Stevenson, *J. Am. Chem. Soc.*, **78**, 546 (1956).

(5) J. W. Mann, *J. Chem. Phys.*, **46**, 1646 (1967).

(6) H. Harrison, D. G. Hummer, and W. L. Fite, *J. Chem. Phys.*, **41**, 2567 (1964).

[†] Materials and Molecular Research Division of the Lawrence Berkeley Laboratory and the Department of Nuclear Engineering, University of California, Berkeley, CA 94720.

[‡] Chemistry Division of the Lawrence Livermore National Laboratory, Livermore, CA 94550.

* Address correspondence to this author at the Department of Nuclear Engineering, University of California, Berkeley, CA 94720.

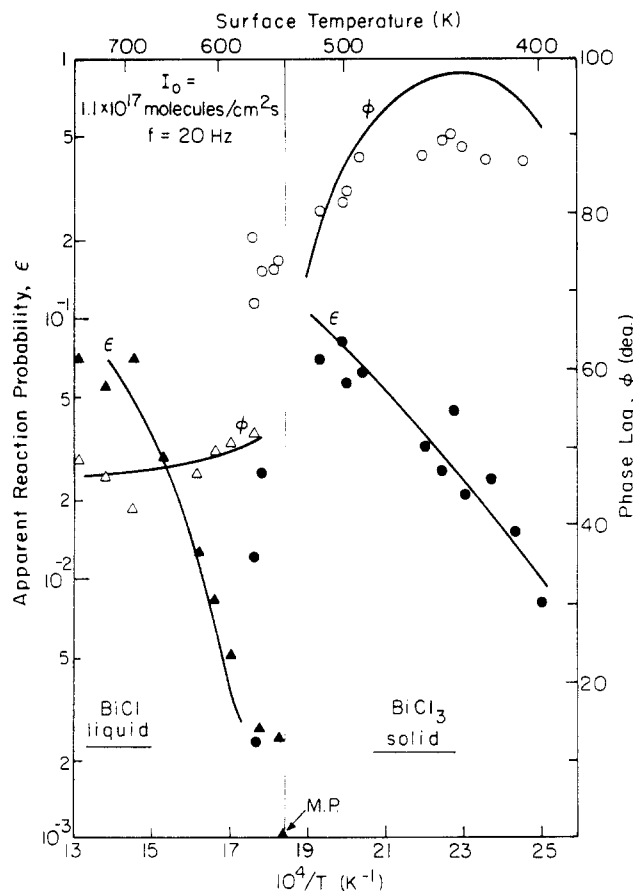


Figure 1. Apparent reaction probabilities and phase lags for BiCl_3 and BiCl as functions of surface temperature. The solid lines are based on a theoretical model.

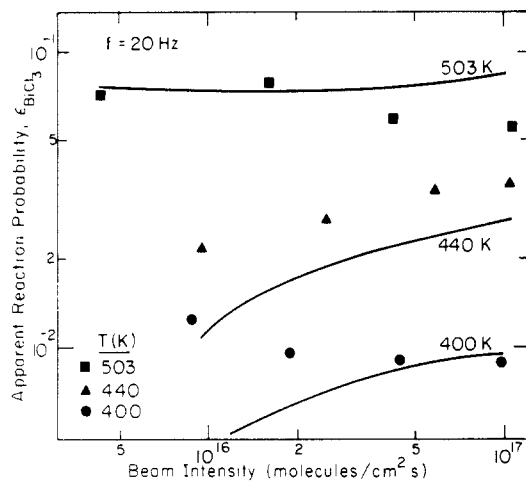


Figure 2. Beam intensity dependence of apparent reaction probability for the BiCl_3 product for three different solid temperatures. The curves are theoretical.

probabilities of BiCl_3 and BiCl do not represent true (dc) reaction probabilities. As will be shown in the following section, the true reaction probability of Cl_2 with solid Bi is temperature independent and equal to the sticking probability.

For the liquid, the BiCl production rate increases rapidly with temperature to 670 K and then shows signs of leveling off, while the phase lag approaches 45° .

The nonlinearity of the reaction at low temperature is seen in the beam-intensity dependences of the phase lag and apparent reaction probability shown in Figures 2 and 3. At 500 K, the apparent reaction probability and phase lag are independent of

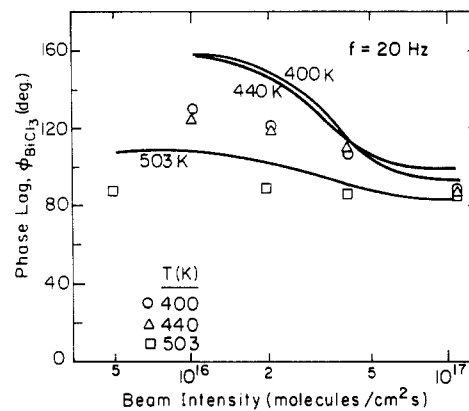


Figure 3. Beam intensity dependence of phase lag of BiCl_3 with respect to scattered Cl_2 for three different solid temperatures. The curves are theoretical.

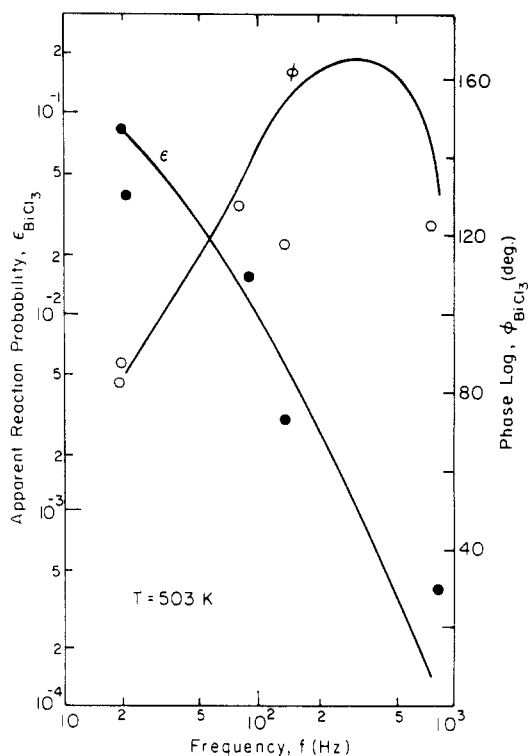


Figure 4. Frequency dependence of apparent reaction probability and phase lag for the BiCl_3 product from solid bismuth. The curves are theoretical.

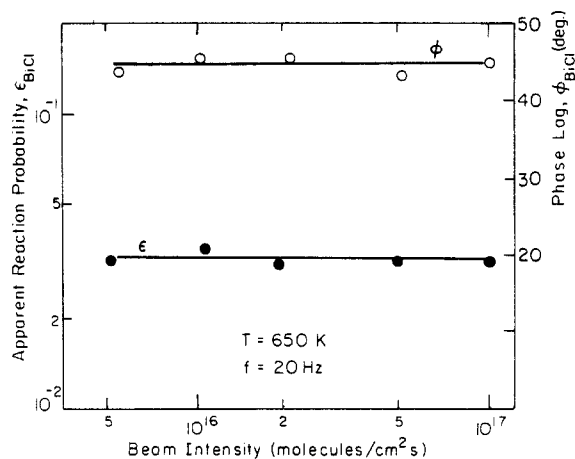


Figure 5. Variations of the BiCl apparent reaction probability and phase lag with beam intensity for liquid Bi . The curves are theoretical.

(7) R. H. Jones, D. R. Olander, W. H. Siekhaus, and J. A. Schwarz, *J. Vac. Sci. Technol.*, **9**, 1429 (1972).

beam intensity, which is characteristic of a linear reaction mechanism.

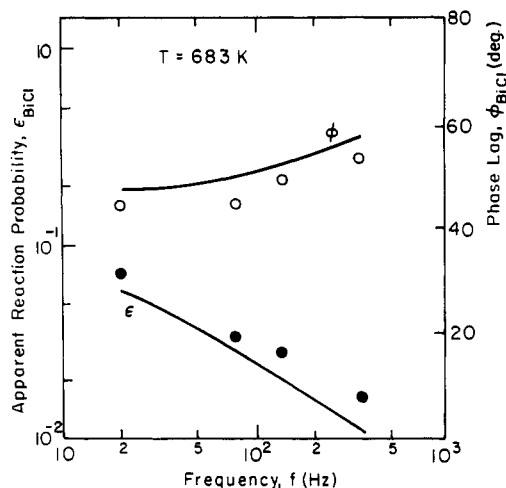


Figure 6. Frequency dependence of the BiCl apparent reaction probability and phase lag for liquid bismuth. The curves are theoretical.

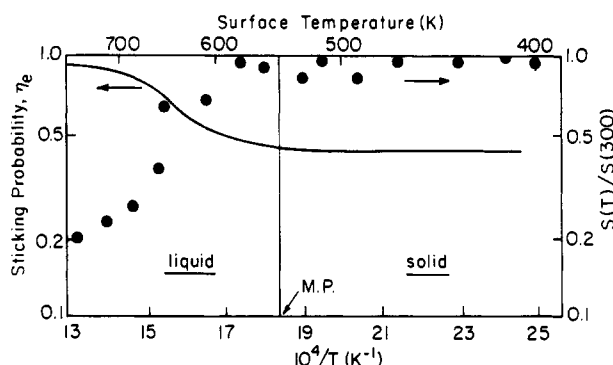


Figure 7. Temperature dependence of the scattered molecular-chlorine signal with respect to that of room temperature. The solid line is the sticking probability deduced for liquid bismuth.

The frequency dependence of the molecular beam data is shown in Figure 4 for solid Bi just below the melting point. The phase lag increases with frequency up to ~ 100 Hz and thereafter remains constant to the maximum attainable chopping frequency of 800 Hz. This insensitivity is usually indicative of a branched step in the mechanism. The phase lags exceed 90° , a result requiring a series mechanism.⁷

The phase lag and reaction probability of the BiCl product of the reaction with liquid bismuth at 650 K shown in Figure 5 are insensitive to incident chlorine beam intensity. The mechanism on the liquid surface therefore consists of first-order processes only.

The phase lag of the BiCl product for the reaction with liquid Bi (Figure 6) increases slowly with frequency, a not unusual observation. However, the low-frequency limit is $\sim 45^\circ$, which occurs when a diffusional process dominates the kinetics.⁷

The temperature dependence of the scattered molecular chlorine signal is shown in Figure 7. A drastic decrease occurs above the melting point due to consumption of chlorine which reappears as the BiCl product. No discontinuity at the melting point is observed in Figure 7, undoubtedly because the difference in chlorine consumption represented by the drop shown in Figure 1 is lost in the scatter of the data in Figure 7. The increase in the BiCl reaction probability for $T > T_{MP}$ shown in Figure 1 and the corresponding decrease in the scattered chlorine signal are attributed to an increase in the Cl_2 sticking probability with temperature of the liquid.

IV. Reaction Model—Solid Bi

Data of Campbell and Taylor.³ The reaction model proposed by Campbell and Taylor (CT, ref 3) dealt only with the desorption of chlorine according to the reaction



They determined the desorption rate constant from steady-state coverage measurements by Auger electron spectroscopy (AES, Figure 6 of ref 3). Their thermal desorption spectroscopy measurements (TDS, Figure 7 of ref 3) were not used in quantitative analysis of the desorption model. In fact, these two sets of measurements cannot be fitted to the model with the same rate constant. We believe, with the concordance of the authors,⁸ that the TDS data are more reliable than the AES data. This conclusion is based upon the following observations. First, the AES data show no evidence of the two distinct binding states (α and β) of chlorine on the Bi(0001) surface. Second, the integrals under the TDS curves of CT's Figure 7 produce a β -state sticking probability which is in good agreement with that measured in Figure 1 of their paper.¹⁴ Third, the coincidence of the three lowest pressure curves in CT's Figure 6 at high temperature cannot be explained by any model, except one which somehow changes to zeroth order at these temperatures. Even though this coverage region was avoided in CT's data-fitting process, vestiges of the unknown experimental problem causing this behavior may have affected the AES signals in the coverage region which they used to extract model parameters from the data. Therefore, we have reanalyzed CT's thermal desorption spectra and deduced numerical values of the rate constant k_d of eq 1 in the process.

Campbell and Taylor³ demonstrated the existence of two binding states of chlorine on Bi(0001). The weakly bound α state constitutes an overlayer on the β -state chlorine, which is attached directly to the crystal surface and which desorbs according to eq 1. The β state is the sole surface species present at coverages below ~ 0.3 . Thus, the TDS curves a, b, and c in CT's Figure 7 reflect the behavior of this state only, with no interference from α -state desorption. Our molecular beam data, although obtained under equivalent chlorine pressures higher by about 2 orders of magnitude, also represent higher crystal temperatures than used by CT. We estimate that the average chlorine coverage of the Bi surface during the molecular beam experiments was for the most part less than 0.3, and thus the data reflect behavior of the β state; only the data at the lowest surface temperatures and highest beam intensities are likely to have been influenced by the presence of α -state chlorine.

Consequently, the temperature and coverage dependences of the rate constant k_d in eq 1 were determined from the a, b, and c curves in CT's Figure 7 after removal of background from the spectra. Theoretical spectra were determined by numerically integrating the desorption rate equation

$$dn/dt = -k_d n \quad (2)$$

where³

$$k_d = k_{d0} \exp[-E_0(1 - g\theta)/RT] \quad (3)$$

The initial condition is

$$n(0) = n_{\text{max}}\theta_0 \quad (4)$$

where θ_0 is the initial coverage (ranging from 0.04 to 0.17 for the a-c curves in CT's Figure 7) and $n_{\text{max}} = 1.57 \times 10^{15} \text{ cm}^{-2}$ is the maximum monolayer packing density of adatoms on the (0001) face of bismuth.

In these equations, n is the surface concentration of β -state chlorine and $\theta = n/n_{\text{max}}$ is the fractional coverage. The preexponential factor k_{d0} , the zero-coverage binding energy E_0 , and the coverage sensitivity factor g were determined by fitting CT's data to the integral of eq 2.¹⁵

A Monte Carlo method was used in obtaining the best fit of the model to the data, which yielded the following parameter values:

$$k_{d0} = 6.6 \times 10^{13} \text{ s}^{-1}$$

$$E_0 = 27 \text{ kcal/mol}$$

$$g = 0.33$$

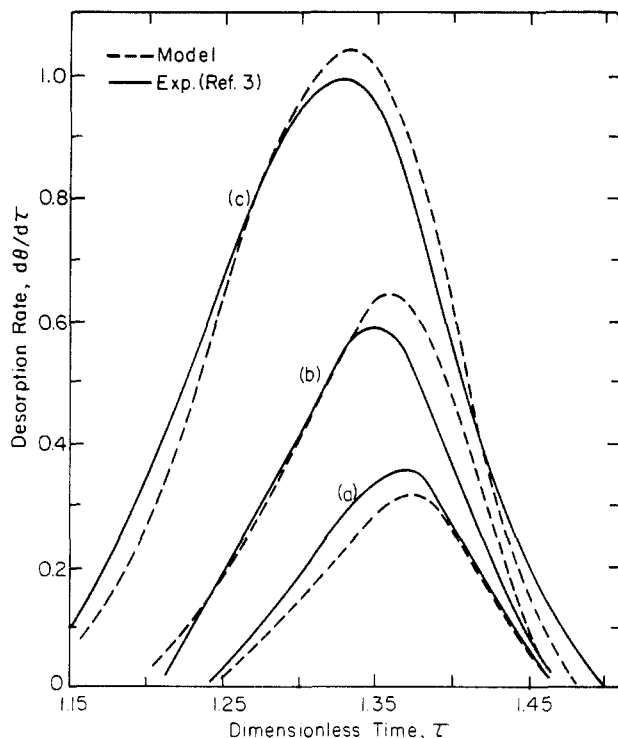
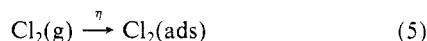


Figure 8. Comparison of Campbell and Taylor's experimental TDS data (with background removed) with the best fit to the coverage-dependent activation energy model. $\tau = T/300$ is the dimensionless crystal temperature, which is a linear function of time (6.9 K/s ramp rate). a, b, and c denote the spectra with the same labels in Figure 7 of ref 3.

The resulting best fit thermal desorption spectra and the experimental curves are compared in Figure 8. The parameter values deduced in the manner described above are not too different from those obtained by CT in fitting the same model to their AES data (i.e., those in Figure 6 of ref 3). However, no set of three parameters provides an adequate fit to both the AES and TDS data simultaneously, and the set given above is more reliable.

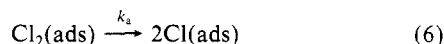
Steps in the Reaction Model. The results obtained in the preceding section were used without alteration in analyzing the molecular beam results. However, the conditions of the molecular beam experiment differ from those of the TDS experiments in that desorption of BiCl_3 takes place during reactant Cl_2 impingement, so elementary reaction steps in addition to the desorption step of eq 1 have to be considered.

The first step is sticking of Cl_2 to the surface to form a molecular precursor state

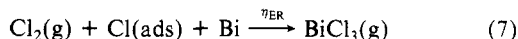


In accord with CT's results, the sticking probability η is assumed to be coverage independent for $\theta < 0.3$. However, nothing is known from their study of the temperature dependence of η . Nor is it known whether the above reaction is reversible.

The second step in the model is slow chemisorption of the precursor to produce β -state adatoms:



Finally, the model provides a parallel pathway for reaction product formation by the Eley-Rideal mechanism:



where η_{ER} is the probability that an incident Cl_2 molecule which strikes a chlorine adatom will also react with it (instantaneously) to produce the volatile bismuth chloride which immediately leaves the surface.

Equations 1 and 5–7 constitute the model. In its simplest form it has three adjustable parameters, namely, the preexponential factor and the activation energy of k_a , and η_{ER} . The remaining

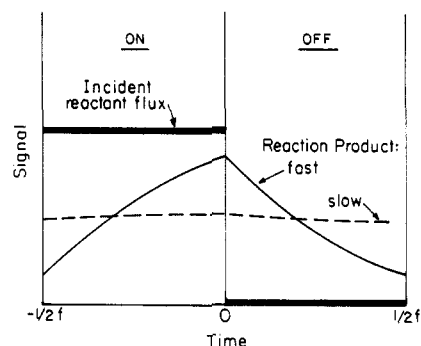


Figure 9. Responses of the surface concentration of reaction intermediate to a square-wave modulated incident reactant flux.

parameters (η and k_a) are taken directly from the preceding analysis of the Campbell-Taylor data. Additional complexities, including a temperature-dependent sticking probability in eq 5, and inclusion of the reverse reactions of eq 5 and 6, were not needed to obtain reasonable agreement of the model predictions and the data.

Analysis of the Molecular Beam Data. Because of the strong nonlinearity contained in the coverage dependence of the BiCl_3 desorption rate constant (eq 3), the usual data analysis technique of linearizing the surface mass balances⁹ is of questionable applicability. Alternatively, the exact but more tedious procedure described in ref 10 is used.

In this method, the incident reactant beam is assumed to be chopped into a perfect square wave of frequency f . The intensity of the beam during the "on" portion of the cycle is I_0 and zero during the "off" half of the cycle. This square-wave incident flux and two waveforms representing schematically the concentration of a surface species under different experimental conditions are sketched in Figure 9. The shapes of the latter must be calculated by integrating the surface mass balance for the species in question and fixing the integration constants by requiring that the concentrations at the beginning and the ends of each cycle be equal. These matching conditions reflect the periodic nature of the waveforms. The two product waveforms shown in Figure 9 represent extreme cases: one which is relatively responsive to the driving square wave of the incident reactant flux and another representing a sluggish reaction which gives a nearly flat waveform. The latter type of waveform produces a very large phase lag when analyzed by lock-in amplification. For the reaction model described earlier, these general considerations take the following quantitative form.

The surface balance on the physisorbed Cl_2 (coverage θ_a) is obtained from eq 5 and 6 as

$$\text{beam on: } d\theta_a^{\text{on}}/d\tau = Q - K_a\theta_a^{\text{on}} \quad (-1 \leq \tau \leq 0) \quad (8)$$

$$\text{beam off: } d\theta_a^{\text{off}}/d\tau = -K_a\theta_a^{\text{off}} \quad (0 \leq \tau \leq 1) \quad (9)$$

where τ , Q , and k_a are dimensionless time, beam intensity, and chemisorption rate constant, respectively:

$$\tau = 2ft$$

$$Q = \frac{\eta I_0}{2fn_{\text{max}}}$$

$$K_a = k_a/2f$$

The matching conditions required by waveform periodicity are

$$\theta_a^{\text{on}}(0) = \theta_a^{\text{off}}(0)$$

$$\theta_a^{\text{on}}(-1) = \theta_a^{\text{off}}(1) \quad (10)$$

(9) A. Ullman and D. R. Olander, *Int. J. Chem. Kinet.*, **8**, 625 (1976).

(10) D. R. Olander in *The Structure and Chemistry of Solid Surfaces*, G. A. Somorjai, Ed., Wiley, New York, 1969.

TABLE I: Parameters of the Bi/Cl₂ Reaction

parameter	preexponential factor	activation energy, kcal/mol
Solid Bismuth		
η	0.43 ^a	
η_{ER}	4×10^{-3}	
k_d	$6.6 \times 10^{13} \text{ s}^{-1}$	27(1 - 0.33 θ)
k_a	$1.7 \times 10^5 \text{ s}^{-1}$	8.4
Liquid Bismuth		
η_l	0.43-0.9 ^b	
k_1	$5 \times 10^7 \text{ s}^{-1}$	19
H^2D	10^4 s^{-1}	~0

^a Obtained by fitting the TDS data of ref 3. ^b See Figure 7.

The surface balance on chemisorbed chlorine atoms, with coverage θ , results in

beam on:

$$d\theta^{on}/d\tau = 2K_a\theta_a^{on} - K_d\theta^{on} - \frac{\eta_{ER}}{\eta}Q\theta^{on} \quad (-1 \leq \tau \leq 0) \quad (11)$$

$$\text{beam off: } d\theta^{off}/d\tau = 2K_a\theta_a^{off} - K_d\theta^{off} \quad (0 \leq \tau \leq 1) \quad (12)$$

where

$$K_a = k_d/2f \quad (13)$$

The first term on the right-hand side of the eq 11 represents the production of Cl(ads) from dissociation of physisorbed Cl₂. This term is evaluated from the analytical solutions of eq 8 and 9. The second term is the loss due to reaction 1 with the coverage-dependent rate constant k_d (eq 3). Following Campbell and Taylor, this step is taken to be first order in the adsorbed chlorine concentration. The last term is the loss due to product formation by the Eley-Rideal mechanism (eq 7).

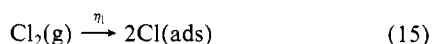
The matching conditions for the chemisorbed chlorine atom waveform are

$$\begin{aligned} \theta^{on}(0) &= \theta^{off}(0) \\ \theta^{on}(-1) &= \theta^{off}(1) \end{aligned} \quad (14)$$

Numerical solutions of eq 11 and 12 are obtained and from these the BiCl₃ desorption rate waveform is calculated. The magnitude of the first Fourier component of the product waveform with respect to that of the reflected Cl₂ beam (i.e., the apparent reaction probability, ϵ_{BiCl_3}) and the phase lag, ϕ_{BiCl_3} , are calculated¹⁰ and compared with the experimental results. The values of K_a and η_{ER} which provide the best agreement between model and experiment are determined by a least-squares computational method. The results of the fitting of the molecular beam data as well as the TDS data of ref 3 are shown in Table I. Comparisons of the model with the molecular beam data are shown as solid curves in Figures 1-4.

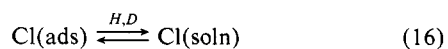
V. Reaction Model—Liquid Bi

The following model is based upon two salient features of the experimental results. First, the linearity of the reaction and second the dominating influence of diffusion into the liquid, as evidenced by the near-45° phase lag of the BiCl product. Fast transfer between the adsorbed molecular precursor state of chlorine to the chemisorbed state is assumed because nothing in the data suggests that anything more refined is necessary. Thus, adsorption is equivalent to direct dissociative chemisorption of gaseous chlorine on the surface of the liquid. This step is expressed by



where η_l is the sticking probability.

The remaining elementary reaction steps are solution diffusion in the bulk liquid



which competes with the surface reaction forming the only observed product



Reaction 16 represents dissolution of chlorine atoms with solubility coefficient H and migration with diffusivity D into the liquid. Reaction 17 denotes the production and desorption of bismuth monochloride.

Explicit solutions for the apparent reaction probability and the phase lag obtained by the conventional analysis method are

$$\begin{aligned} \phi_{BiCl} &= \tan^{-1} \left[\frac{\frac{2\pi f}{k_1} + \frac{H}{k_1}(\pi f D)^{1/2}}{1 + \frac{H}{k_1}(\pi f D)^{1/2}} \right] \\ \epsilon_{BiCl} &= \left[\frac{2\eta_l}{1 + \frac{H}{k_1}(\pi f D)^{1/2}} \right] \cos \phi_{BiCl} \end{aligned} \quad (18)$$

Equations 17 and 18 contain the three parameters of the reaction models, namely, k_1 , H^2D , and η_l .

For solid Bi, satisfactory fitting of the reaction model to the molecular beam data was accomplished with a temperature-independent sticking probability of 0.43, which is the value deduced from Campbell and Taylor's TDS data. However, as indicated at the end of section III, the decrease in the scattered Cl₂ signal (Figure 7) and the increase in the BiCl product signal (Figure 1) as the temperature is raised above the melting point of bismuth are viewed as manifestations of a corresponding increase in the Cl₂ sticking probability. Since the signal due Cl₂ reflected from the surface (S) is proportional to 1 minus the sticking probability, we have

$$\eta_l(T) = 1 - 0.57 \frac{S(T)}{S(300)} \quad (19)$$

where $S(T)$ and $S(300)$ are the reflected chlorine signals from the liquid surface at temperatures T and 300 K, respectively. Equation 19 is plotted in Figure 7. The chlorine sticking probability on the liquid increases from the value on the solid at the melting point to approximately 0.9 at 770 K.

The values of the remaining parameters which provide the best agreement between the model and the data were obtained by least-squares computational methods using the data in Figures 1, 5, and 6. The results of the fitting process are summarized on the bottom of Table I and comparisons of the theoretical reaction product vector (i.e., eq 18) with the data are shown as curves in Figures 1, 5, and 6.

VI. Discussion and Conclusions

A combination of surface techniques, including LEED, AES, TDS, and, in the present work, modulated molecular beam mass spectrometry, have been brought to bear on the reaction of molecular chlorine with single-crystal bismuth. Campbell and Taylor's AES and LEED measurements provided information on adsorbate concentration and structure and their thermal desorption spectroscopy measurements gave quantitative kinetic information on product desorption rates. The molecular beam data reported in this work contain information on the combined processes of adsorption, surface reaction, and desorption; mass spectrometric detection unambiguously identified the reaction product.

The very sluggish change in reaction product phase lag with temperature and with modulation frequency is explicable only if the reaction mechanism contains parallel paths of different rates which form the same reaction product (BiCl₃ in this case). In the proposed model, one of these paths is the Langmuir-Hinshelwood (LH) step identified by Campbell and Taylor³ by which three chlorine adatoms simultaneously abstract a bismuth surface atom and form the trichloride product in a first-order process. The parallel path, which is not detectable in TDS experiments,

is the Eley-Rideal (ER) step involving collision of an impinging Cl_2 molecule with a chlorine adatom which together remove a bismuth atom from the surface. Reaction product formation by this branch is no more than 1% of that by the LH step, but the existence of the ER step is inferred from the molecular beam data under conditions which strongly demodulate the BiCl signal from the LH process (i.e., at low temperatures or high modulation frequencies). Eley-Rideal steps in chlorine reactions with solids appear to be relatively common, having been observed previously for lead² and iron.¹¹ For all three of these systems, the ER step is temperature independent.

The Bi/Cl_2 reaction is unusual because the reaction product appears with very large phase lags relative to the incident chlorine flux. Phase lags exceeding 90° , which were observed in this study, can only be explained by a series process in the mechanism. In the present reaction model for the solid, this feature is embodied in the two-step adsorption process which precedes product formation. Creation of the physisorbed state from the impinging Cl_2 is instantaneous (on the time scale of beam modulation), but the transformation of this state to the chemisorbed β -state chlorine occurs with mean times on the order of milliseconds. This slow step is followed by another slow step, namely, reaction with the substrate bismuth atoms to form product molecules. These two back-to-back slow steps combine to produce phase lags as high as 130° , which means that the waveform trace is practically a horizontal line (see Figure 9). The rate constant for the physisorbed-to-chemisorbed transfer (k_a) has a low preexponential factor and a low activation energy (Table I), suggesting that surface migration to favorable reaction sites may be involved.

A recurring hope in mechanistic modeling of surface reactions is to be able to compare the kinetic parameters with bulk thermodynamic properties of the reacting system, such as heats of adsorption, solution, or reaction. Unfortunately, it is rare that a clear comparison of this type can be made, principally because the kinetic parameters are obtained in highly nonequilibrium conditions. However, when the elementary step in the kinetic model is very simple, such as desorption of a surface-bound species, the numerical parameters of the model can be related to theoretical expectations or to thermochemical information. The preexponential factor of the desorption rate constant for formation of BiCl_3 (k_d), for example, is in the range expected for vibrational frequencies of molecules on the surface. In addition, the activation energy for desorption is expected to be of the order of magnitude of the heat of sublimation of BiCl_3 . The latter is reported to be 28.4 kcal/mol,¹² which compares well with the desorption activation energy of 27 kcal/mol measured here.

(11) M. Balooch, D. R. Olander, and W. J. Siekhaus, *J. Chem. Soc., Faraday Trans. 1*, **80**, 61 (1984).

(12) A. J. Darnell and S. J. Yosim, *J. Phys. Chem.*, **63**, 1813 (1959).

Another point of comparison between equilibrium thermodynamics and the surface reaction is the identity of the product species and its temperature dependence. The equilibrium studies of the vapor species formed by reaction of liquid bismuth with BiCl_3 by Cubicciotti¹³ clearly identified BiCl in the gas phase. In addition, its proportion in the vapor increased with increasing temperature. This observation is in qualitative accord with our finding that the sole reaction product of the reaction of chlorine with liquid bismuth is the monochloride.

In contrast to the In/Cl_2 and Pb/Cl_2 reactions,^{1,2} the Bi/Cl_2 system exhibits a discontinuous change in the kinetics and mechanism of the reaction at the melting point. Of particular interest is the factor of ~ 40 decrease in the reaction probability which accompanies the solid-liquid transition. In addition, when the crystal melts the BiCl_3 product disappears entirely and is replaced by the monochloride product of the reaction with the liquid metal. In the cases of $\text{In}(\text{l})$ and $\text{Bi}(\text{l})$, the reaction products are the monochlorides, whereas in the case of Pb , only the dichloride was found.

Of the three metals studied, the solution-diffusion process most strongly influences the overall reaction in the case of bismuth, while this phenomenon does not appear to be of great importance for indium. Since the diffusivity has a positive activation energy, the zero activation energy observed for the permeability parameter H^2D for chlorine in liquid bismuth means either that both H and D are temperature independent or that solution of surface-adsorbed chlorine in the bulk is exothermic by an amount just equal to one-half of the activation energy for diffusion. Similar behavior was found for liquid lead,² except that the exothermicity of the solubility coefficient H exceeded the activation energy of D , resulting in a negative apparent activation energy for the product H^2D .

Acknowledgment. The authors acknowledge the helpful advice of Dr. Charles Campbell. This work was supported by the Director, Office of Energy Research, Office of Basic Energy Sciences, Materials Sciences Division of the U.S. Department of Energy under Contract No. DE-AC03-76SF00098.

Registry No. Bi, 7440-69-9; Cl_2 , 7782-50-5.

(13) D. Cubicciotti, *J. Phys. Chem.*, **64**, 791 (1960).

(14) The 300 K sticking probability reported by Campbell and Taylor (0.14, ref 3) is a factor of 4 too low because of a numerical error in processing the original data.⁸ The sticking probability obtained from curves a, b, and c of CT's Figure 7 (after removal of background) is 0.43.

(15) To convert the ordinate of Figure 7 of ref 3 to dn/dt , account was taken of the density-sensitive nature of the mass spectrometer detector. The signal is therefore proportional to $(dn/dt) T^{1/2}$, where T is the temperature of the vaporized BiCl_3 , assumed to equal that of the surface. The constant of proportionality was determined by setting the integral of curve f of Figure 7 of ref 3 equal to a coverage of 1.26×10^{15} , as determined by CT in a separate LEED study.